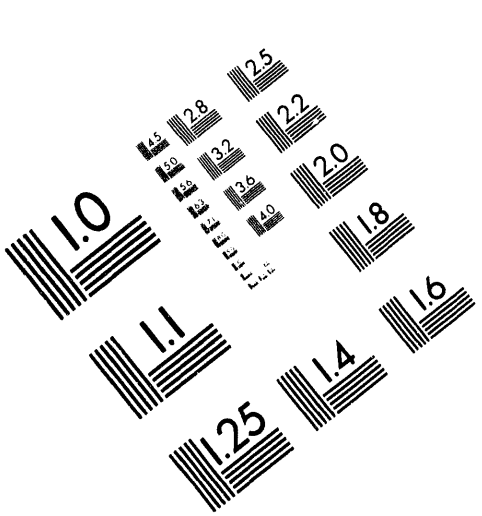

Association for Information and Image Management
1100 Wayne Avenue, Suite 1100
Silver Spring, Maryland 20910
301/587-8202

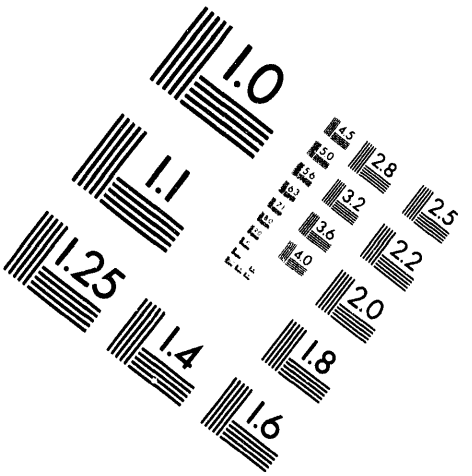

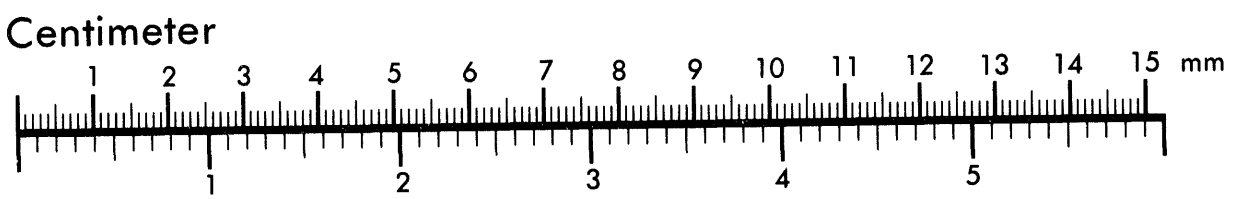

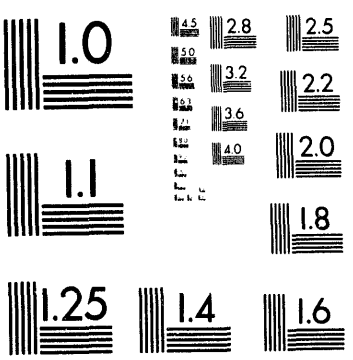

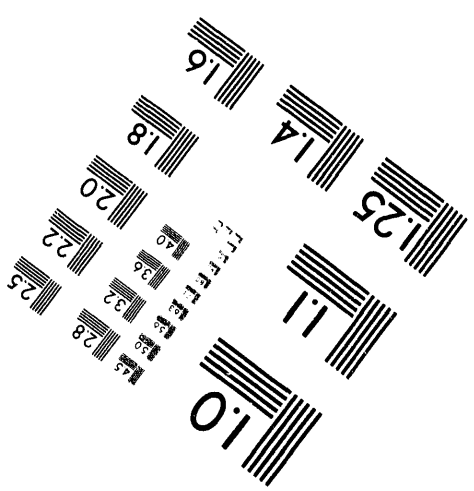

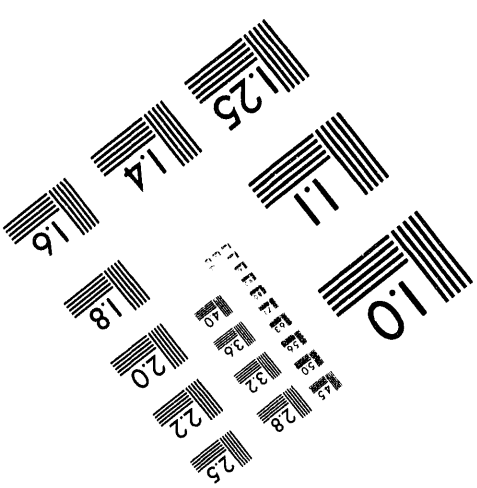

1 of 1

SAND94-0221
Unlimited Release
Printed May 1994

Distribution
Category UC-906

Modified Noise Power Ratio Testing of High Resolution Digitizers

Timothy S. McDonald
J&M Systems, Ltd.
15100 Central Avenue SE
Albuquerque, New Mexico 87123

Sandia Contract No. AB-4486

ABSTRACT

A broadband, full signal range, side-by-side (tandem) test method for estimating the internal noise performance of high resolution digitizers is described and illustrated. The technique involves a re-definition of the traditional Noise Power Ratio (NPR) test, a change that not only makes this test applicable to higher resolution systems than was previously practical, but also enhances its value and flexibility. Since coherence analysis is the basis of this new definition, and since the application of coherence procedures to high resolution data poses several problems, this report discusses these problems and their resolution.

ACKNOWLEDGMENTS

Thanks to the following people for their help: Dick Kromer (9236) for suggesting this revitalization of the NPR test, Joseph Steim (Quanterra, Inc.) for proposing a frequency domain interpolation approach, Sam Stearns (9311) for his guidance concerning the finer points of coherence modeling and analysis and who, along with Bobby Corbell (9236) and Otis Solomon (1042), carefully reviewed the draft of this report, and to Pres Herrington (9236) for his support and encouragement of this effort.

Contents

Figures

Introduction

Estimates of the coherence function have been used for several years in order to characterize the self-noise spectra of seismic sensors [Stearns, 1979, Durham, 1982 and 1987, and Holcomb, 1989, for example]. Although the input signal (ground motion) is generally unknown, the comparison of the sampled output signals (usually measured in volts or digital counts) of two side-by-side seismic sensors by means of the coherence function has provided estimates of these self-noise spectra.

More recently, coherence has been used in the evaluation of the performance of high resolution digitizers (HRD's). Here again the problem is that in most cases the input signal is not adequately defined for more traditional system characterization methods to be used. Since very few signal generators have noise floors below the measurement capability of many of the high resolution digitizers, internal noise due to the digitizer itself is often masked. Fortunately, side-by-side testing and coherence analysis provide a way to estimate internal instrument noise as a function of input signal power for a given digitizer. In addition, the input may be broadband, possibly application-driven signals that span the entire dynamic range of the device. This means that inexpensive, readily obtainable signal generators may be used to evaluate high resolution digitizers so long as at least two of the digitizers are available and may be connected and programmed to convert the same input signal simultaneously (over the same time interval) and at the same sample rate.

Digitizers and System Models

For the purposes of this paper a digitizer is defined to be an instrument that regularly samples a continuous function of time (such as a varying voltage) every T seconds in order to produce a sequence of integers (the samples). An ideal n-bit digitizer is assumed to have the following characteristics:

- The "quantizing step" q is defined as the full-scale input range of the digitizer divided by the number of bit combinations available; e.g., for a 24-bit, ± 20 volt digitizer the quantizing step (or "bit weight") is

$$q = 40.0 \text{ volts} / 2^{24} \approx 2.38 \ \mu\text{volts} \qquad (1)$$

- The input signal at a given sample time is equal to q times the integer sample value to an accuracy of ± q / 2 ("quantizing error"), so long as the input signal is within the range of the digitizer.

- Sample values for input signals beyond the input range of the digitizer are "clipped" to the value for the maximum or minimum signal, as appropriate.

For convenience, samples are assumed to be signed two's-complement integers ("counts") and the input voltage range symmetric with respect to polarity; i.e., the magnitudes of positive and negative full-scale are the same.

The system model used for side-by-side digitizer testing is illustrated in Figure 1. The first digitizer, the "reference" device, is represented by the top branch and the second, the "test" unit, by the bottom branch. Each instrument is modeled as a linear transfer function,

additive linearly-independent noise, and a sampler/digitizer producing integer samples at times t=kT, multiples of the sampling interval T.

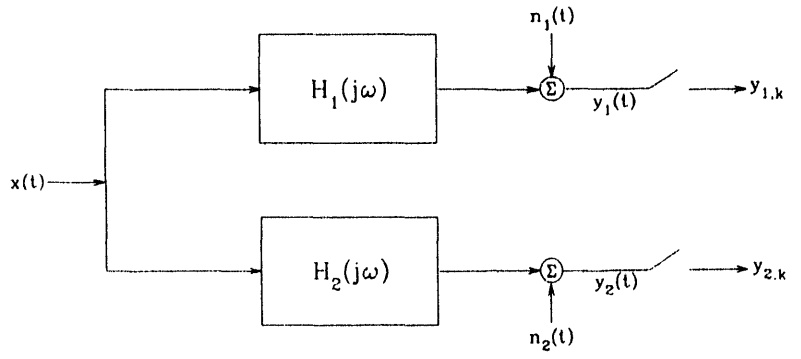

Figure 1 - System Model for Side-by-Side Digitizer Testing

For some purposes it may be appropriate to simplify the Figure 1 model to that shown in Figure 2. [Stearns, 1979, uses these models; Stearns and David, 1993, use slightly different models in which the noise is referred to the input of the transfer functions rather than to the output.]

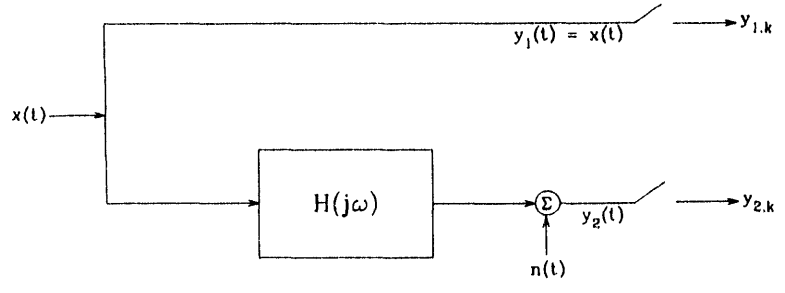

Figure 2 - "Lumped" Noise System Model

Here the two branch transfer functions have been consolidated into H(jω), which provides the linear relationship between the reference and the test channels, and the independent noise functions are "lumped" into the test channel as the single noise function n(t). This model is particularly useful when the system transfer function is already adequately known or is not of interest and the reference device is assumed to be significantly "better" (i.e., demonstrates much lower internal noise) than the instrument under test. Comparison testing against some recognized or assumed standard may utilize this system model.

When the reference and test devices are more or less identical instruments in that one cannot be assumed to be much different from the other, the model illustrated in Figure 3 may be used to provide an estimate of internal noise. The two noise functions, $n_1(t)$ and $n_2(t)$, are assumed to be uncorrelated but of equal power. This is the model used for side-by-side testing of copies of the same device, such as two units of the same digitizer design.

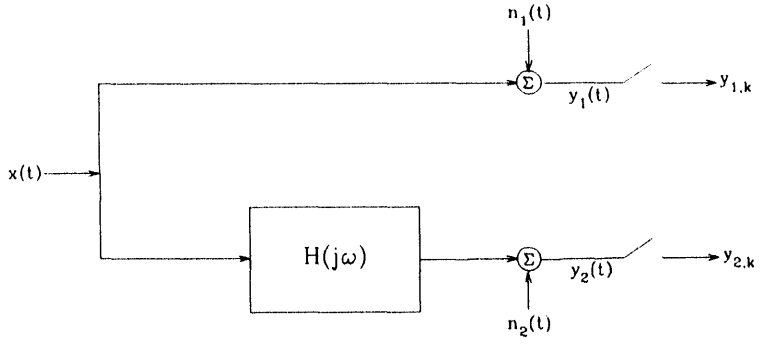

Figure 3 - Distributed Noise System Model

Other system models are possible, of course, and may be appropriate in other special situations [e.g., Holcomb, 1989 and Goldsmith, 1990].

The distributed noise model in Figure 3 is used throughout this study, except for one case in which the lumped noise model in Figure 2 is applicable. The formulas for estimating coherence and related functions for the lumped noise model are developed in a paper by Stearns [1979] and are reproduced here for convenience (with minor changes in notation).

Let $\overline{P}_{y_1y_1}$, $\overline{P}_{y_2y_2}$, and $\overline{P}_{y_1y_2}$ represent estimates of the power spectra of $y_1(t)$, $y_2(t)$, and their cross power, respectively. The mean-squared coherence, which is defined as the ratio of the squared magnitude of the cross power to the product of the individual power spectra, is estimated by

$$\hat{\gamma}^2 = \left|\overline{P}_{y_1y_2}\right|^2 \Big/ \left(\overline{P}_{y_1y_1}\overline{P}_{y_2y_2}\right) \quad (2)$$

The noise power estimate for the lumped noise model is

$$\overline{P}_{nn} = \overline{P}_{y_1y_2}\left(1-\hat{\gamma}^2\right) \quad (3)$$

and the estimate of the linear transfer function $H(j\omega)$ is

$$\hat{H} = \hat{\gamma}^2\,\overline{P}_{y_2y_2} \Big/ \overline{P}^*_{y_1y_2}\ , \quad (4)$$

where the star denotes the complex conjugate.

For the distributed noise model the coherence is still estimated by Eq. (2), but the transfer function and noise power estimates are somewhat different. Assume that the two noise functions have equal power but are uncorrelated, i.e.,

$$P_{n_1n_1} = P_{n_2n_2} \equiv P_{nn} \tag{5}$$

and

$$P_{n_1n_2} = 0 \, . \tag{6}$$

Letting capital letters represent the Fourier transforms (or z-transforms) of the corresponding lower case time functions (or sample sets) and omitting the frequency (or z) dependency for the sake of brevity, the top and bottom branches in Figure 3 yield

$$Y_1 = X + N_1 \tag{7}$$

and

$$Y_2 = XH + N_2 \, . \tag{8}$$

The basic estimates of power spectra and cross power spectra require scaling and averaging operations in order to provide meaningful coherence results. All the spectra used for this study were obtained by periodogram averaging, a technique attributed to Welch [1967], and are scaled to compensate for windowing (Hann window), five-eighths overlapping [Carter, et. al., 1973 and Stearns, 1981], Fast Fourier Transform (FFT) size, sampling interval, and power at negative frequencies. A bar over equation elements represents this (or some other) averaging and scaling operation. The cross power estimate for the distributed noise model is given by

$$
\begin{aligned}
\overline{P}_{y_1y_2} &= \overline{\left(Y_1^* Y_2\right)} \\
&= \overline{(X + N_1)^*(XH + N_2)} \\
&= \overline{\left(X^* XH + X^* N_2 + N_1^* XH + N_1^* N_2\right)} \\
&= \overline{P}_{xx} \hat{H}
\end{aligned}
\tag{9}
$$

The last line follows since the noise functions are assumed to be uncorrelated with each other and with x(t). Similar analysis for the individual channel power estimates yields

$$
\begin{aligned}
\overline{P}_{y_1y_1} &= \overline{\left(Y_1^* Y_1\right)} \\
&= \overline{(X + N_1)^*(X + N_1)} \\
&= \overline{\left(X^* X + X^* N_1 + N_1^* X + N_1^* N_1\right)} \\
&= \overline{P}_{xx} + \overline{P}_{nn}
\end{aligned}
\tag{10}
$$

and

$$
\begin{aligned}
\overline{P}_{y_2y_2} &= \overline{\left(Y_2^* Y_2\right)} \\
&= \overline{(XH + N_2)^*(XH + N_2)} \\
&= \overline{\left(X^* XH^* H + X^* N_2 H^* + N_2^* XH + N_2^* N_2\right)} \\
&= \overline{P}_{xx} \left|\hat{H}\right|^2 + \overline{P}_{nn} .
\end{aligned}
\tag{11}
$$

Solving Eqs. (9) through (11) for the noise power and transfer function estimates for the distributed noise model produces

$$
\overline{P}_{nn} = \tfrac{1}{2}\left(\overline{P}_{y_1y_1} + \overline{P}_{y_2y_2}\right) - \sqrt{\tfrac{1}{4}\left(\overline{P}_{y_1y_1} - \overline{P}_{y_2y_2}\right)^2 + \left|\overline{P}_{y_1y_2}\right|^2}
\tag{12}
$$

and

$$
\hat{H} = \overline{P}_{y_1y_2} \Big/ \left(\overline{P}_{y_1y_1} - \overline{P}_{nn}\right) .
\tag{13}
$$

Note that the transfer function is a complex function of frequency and that noise power is real. The transfer function is often presented as a pair of real functional estimates, power gain and phase:

$$\left|\hat{H}\right|^2 = \hat{H}^* \hat{H} \tag{14}$$

and

$$\Theta = \tan^{-1}\left[\mathrm{Im}\left(\hat{H}\right) / \mathrm{Re}\left(\hat{H}\right) \right], \tag{15}$$

where Im() refers to the imaginary part of its complex function argument and Re() to the real part.

Sample Timing and Time-Invariance

It is well known that the estimates for signal power and cross power as described earlier are biased. Carter and Nuttall [1976] discuss two sources of the biasing. The first stems from the underlying assumption (which is never completely satisfied in the real world) that each FFT segment used in the spectral estimation procedure is long enough to ensure complete spectral resolution. However, when coherence is close to unity, as it must be for our purposes, and when the input signal spectrum does not have sharp peaks or tonals, this source of biasing has a negligible effect.

A second source may cause serious problems if not properly handled: biasing of the cross power estimate due to signal misalignment [see also Carter, 1980]. This may be thought of as a constant time shift between the samples in one set relative to the other or as a linear phase relationship in the transfer function; the views are equivalent. While most users of digital coherence techniques are aware of this requirement, it has usually been sufficient to align the two sample sets by shifting one set sample-by-sample to the point of maximum cross-correlation with the other sample set. For the extremely high signal-to-noise ratios (SNR's) involved in HRD evaluation, this technique is no longer adequate; alignment must be accurate and consistent to a small fraction of the sampling interval. Stearns has shown in an unpublished study that the bias due to misalignment is dependent on the size of the time shift and on the spectrum of the input signal, but that for highly coherent signals this biasing is largely correctable by post-processing the results of the coherence analysis. Another method of compensating for misalignment is to perform an interpolation of one sample set in order to align it with the other set. Care must be taken that the interpolation method preserves the spectral content of the data. This suggests a frequency domain scheme such as the one described in the next section.

However, it is important to keep in mind other assumptions and requirements concerning this evaluation procedure. For HRD evaluation and other high SNR applications of coherence analysis, signal timing becomes extremely important. The requirement that the sample sets be obtained synchronously (at the same sample rate) and simultaneously (over the same time interval) may be interpreted to allow for a constant time shift between signals or other correctable sample time characteristics, but the emphasis must be on the concept that the timing be correctable. For instance, the case in which the two digitizers being tested have independent sampling clocks that, while very regular, have known but slightly different frequencies may be a timing situation that (conceivably) can be corrected. On the other hand, errors due to random timing jitter are not correctable.

Another underlying assumption is that the digitizers are not time-varying devices (or, at least, that their response characteristics do not change significantly during a data acquisition period). Test procedures involving warm-up periods for electronic equipment and/or a constant-temperature environment for the testing may be required so that this assumption is not significantly violated. Inconsistency of results or an increasing internal noise level with longer (time duration) tests could indicate a problem in this area.

Frequency Domain Interpolation

A common characteristic of multiple-channel digitizer systems is that a constant, usually small timing difference exists between channels. In other words, analog-to-digital conversions take place at slightly different times on the various data channels, although the sample rate is the same for all channels and the difference between conversion times for any pair of channels is essentially constant. This condition presents a problem for coherence analysis, since the cross-power estimation is sensitive to timing differences between sample sets.

This time difference (if it exists) can be removed by interpolating between the samples in one of two sample sets to obtain new samples that are essentially simultaneous with the those in the other set. However, the choice of interpolation scheme is important. Since our analysis is based on frequency-domain techniques, it is vital that the interpolator chosen preserve the frequency content of the original sample set. The common linear and polynomial-based interpolation methods are generally not adequate for these purposes. Preservation of frequency-domain characteristics while performing time-domain linear operations is an area that often requires special considerations [McDonald, 1977 and Stearns and Hush, 1990]. The scheme used herein is fairly straightforward and stems from the relationship for non-aliased discrete Fourier transforms (DFT's) that, if $\overline{F}(j\omega)$ is the DFT of the set $[f(nT)]$, then the DFT of a synchronous but not simultaneous set $[f(nT+\tau)]$ is $e^{j\omega\tau}\overline{F}(j\omega)$.

A constant sampling time difference can be removed from one set of unaliased data samples while preserving the frequency content by the following steps:

1. Determine the constant time difference τ between two sets of data samples. It is assumed that $\tau<T$, the sampling interval, so that the two sample sets cover the same time interval to within a single sample time. If the input data is broadband, a close

approximation of the time difference can be obtained from the slope of the linear phase shift in the transfer function from a preliminary coherence analysis, as shown in the example below.

2. If the DFT size is N samples, center the N samples to be interpolated (say, y_k to y_{k+N-1}) in an array of size 2N with the appropriate samples from the input sequence in the preceding N/2 and following N/2 samples (i.e., the array would contain samples $y_{k-N/2}$ to $y_{k+3N/2-1}$). Windowing should not be necessary for this operation, but if it is used, take care that the middle "N plus a few" samples are windowed with the same constant value (usually 1).

3. Take the DFT of the 2N-sample array. (This discussion assumes a complex DFT operation. Many commercial analysis packages realize the DFT by a Fast Fourier Transform (FFT) subroutine which often assumes a real rather than complex time sequence and yields only half as many complex transform values. The adaptation of this procedure to such software tools should be straightforward.)

4. Multiply the 2N complex DFT values by $e^{-j\omega_n r}$. Note that the nth (n=0, 1, 2, ..., 2N-1) DFT value is associated with a specific angular frequency; i.e., $\omega_n = \pi n/NT$ radians/second for $0 \le n \le N$ and $\omega_n = \pi(2N - n)/NT$ for $N < n < 2N$.

5. Perform an inverse-DFT on the result. The middle N values are the desired interpolated samples.

The double-sized DFT's are used in order to avoid the troublesome edge effects on the first and last few sample values due to DFT and inverse-DFT computation. Usually these effects are reduced by data windowing, but in this case windowing and the subsequent inverse-windowing would result in some "near-zero-over-near-zero" problems around the

ends of the sample set. By doubling the DFT size and moving the samples of interest to the middle, the edge effects are shifted to samples that are not needed.

One point which should be emphasized here and whenever high-precision data is processed by computer is that the analyst must be aware of the effects of internal computer floating-point representation roundoff and truncation errors. The common single precision (4 byte floating-point) representations provide only about 25 bits of mantissa and thus are not adequate for data processing involving multiplications of high resolution digitizer samples. Double precision (8 byte floating-point) is usually implemented with a mantissa of over 50 bits, which is sufficient for our purposes.

Throughout this paper, N is required to be a power of 2 and a complex-valued Fast Fourier Transform (FFT) algorithm is used to obtain the DFT values. The distributed noise model (Figure 3) is used for calculating the coherence-related functions.

An example that illustrates the problems that arise from a fairly small time shift and the results of the above method uses actual data files from a 24-bit format digitizer. The sample rate is 40 samples/second (sampling interval T=0.025 seconds) on each channel and the time difference between channels 1 and 2 is approximately 70 microseconds, or about 0.3% of the sampling interval. A total of 32,000 samples were acquired from each digitizer channel. Spectra were estimated using a Hann window, an FFT size of 512 points, and 5/8 segment overlapping; this means each spectrum is the average of 165 transforms.

Both data channels are connected to a broadband signal source (Gaussian white noise generator) with power spectral density shown in Figure 4. Coherence analysis yields the graph in Figure 5 of the transfer function phase angle and that in Figure 6 of the internal noise power. The slope of the line approximating the phase angle over the frequency range of significant signal power and high coherence (0 to about 19 Hz) in Figure 5 is

$$0.252°/10\,\text{Hz} = [0.252°/(360°/\text{cycle})]/10\,\text{cycles / second} = 70\ \mu\text{seconds}.$$

This value is used in interpolating the data set for channel 2 to match the sample times for channel 1. The results are shown in Figure 7 which illustrates that the residual time discrepancy is negligible (and may be further reduced by iterating the interpolation procedure) and in Figure 8, which shows that the estimated internal noise is 20 dB lower over most of the frequency range than that shown in Figure 6. It should be noted that the results in Figure 8 match very closely those obtained by two other methods: (1) the use of very large values of N for the FFT, which also reduces the bias in the cross-power estimate, and (2) using another channel pair. (Two of the four channels in this system were sampled essentially simultaneously, and all channels were expected to have similar internal noise levels.)

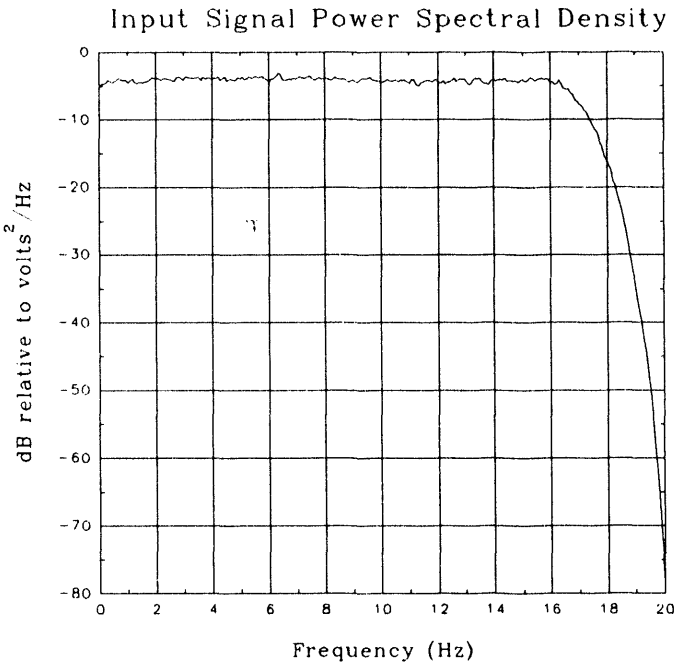

Figure 4 - Common Input Signal Spectrum

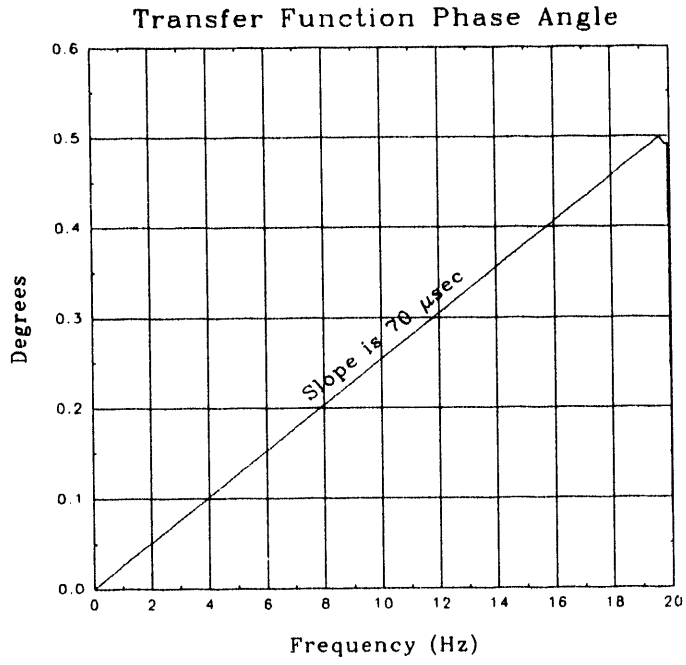

Figure 5 - Transfer Function Phase Angle before Interpolation

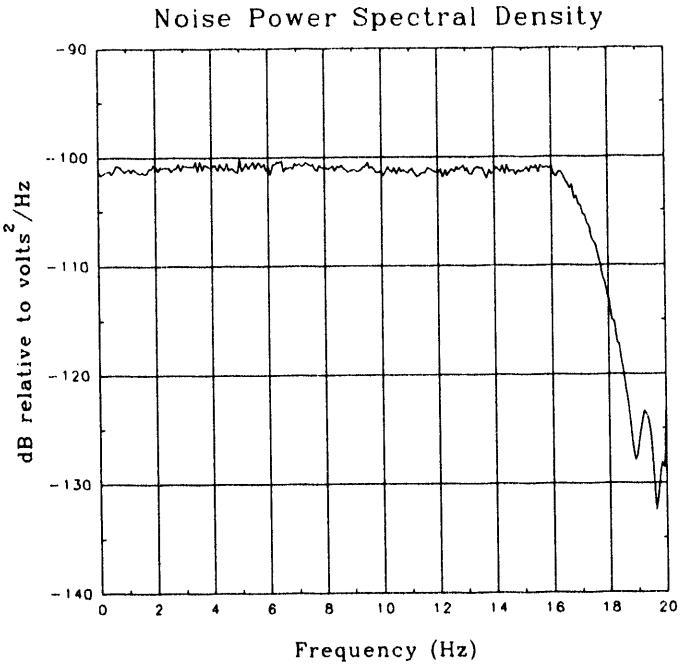

Figure 6 - Internal Noise Power Estimate before Interpolation

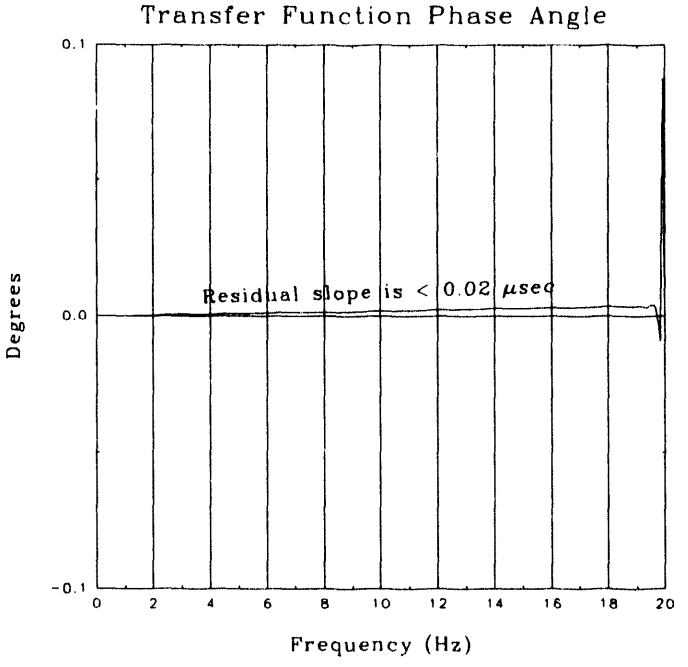

Figure 7 - Transfer Function Phase Angle after Interpolation

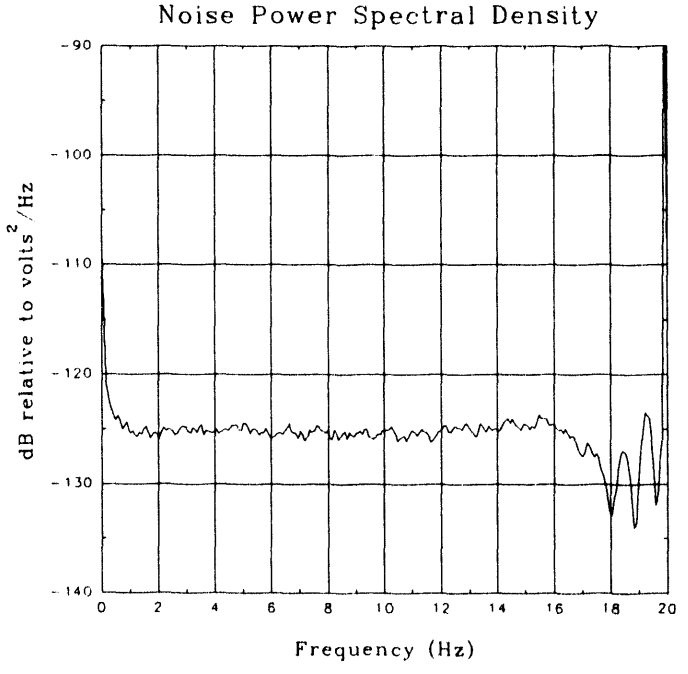

Figure 8 - Internal Noise Power Estimate after Interpolation

Noise Power Ratio

The measurement of Noise Power Ratio (NPR) has been used fairly extensively as a metric for the transmission characteristics of Frequency Division Multiplexed (FDM) communications systems [see Freeman, 1981, and Kester, 1989]. Its purpose is to measure internal noise as broadband input signal levels vary. The concept is fairly simple and is depicted graphically in Figure 9. A broadband Gaussian signal source (such as the one whose spectrum is shown in Figure 4) is connected to a narrow band-stop or "notch" filter, which may be switched in or out. This combination is used as the system input, and measurements of system output signal power at the notch filter center frequency are made both with and without the notch filter being used. The ratio of these two power levels is the NPR and is usually expressed in dB. (Many readers will recognize this as the signal-to-noise ratio; the "Noise Power Ratio" terminology stems from the fact that the "signal" is traditionally supplied by a "noise" generator.)

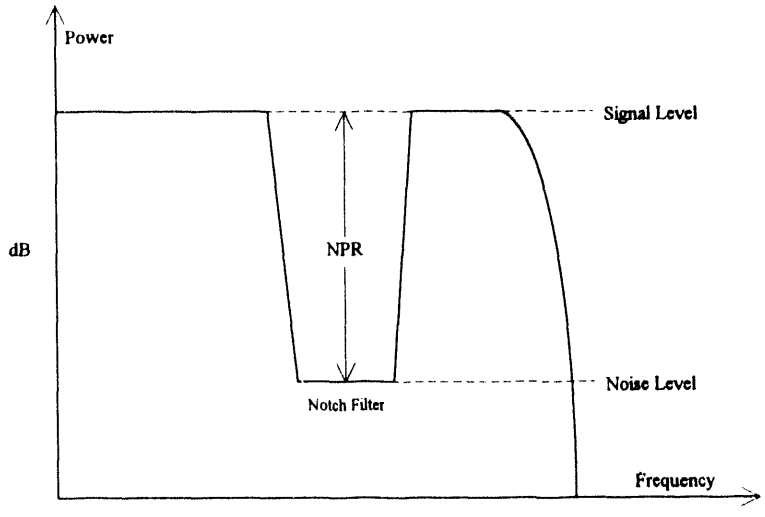

Figure 9 - Noise Power Ratio Measurement (Traditional)

This technique has been used to evaluate the performance of digitizers by comparing NPR values at several signal levels to the NPR curves for ideal n-bit systems [Gray and Zeoli,

1971], but such testing is limited to fairly low resolution systems due to the relatively poor rejection levels of most notch filters. (For high resolution digitizers, the internal noise may be significantly below the "bottom" of the notch and thus not measurable by this procedure.)

Coherence analysis provides a way around the use of a notch filter, thereby providing a new approach for estimating the NPR. Since two of the spectra that may be computed during coherence estimation are signal and noise power densities, these may be integrated over an appropriate frequency interval to provide the signal and noise power values for the NPR, which is signal power divided by noise power. This redefined test can be an important tool for measuring the broadband (and possibly application driven) performance of high resolution digitizers. While traditional NPR methods measure performance at a single frequency (the middle of the notch) at a time, the coherence approach is by its very nature broadband. In addition, the frequency content of the input signal and the integration interval for the power density spectra may be designed or chosen to match some application parameters or specialized test criteria.

Application of NPR to digitizers involves a "loading factor," usually denoted by the letter K, which represents the ratio of the full-scale voltage range for the digitizer to the RMS signal voltage. The curves for the ideal n-bit systems [Gray and Zeoli, 1971] are derived from the assumption that the noise sources are limited to quantization noise (dominant at low to moderate signal levels),

$$\text{quantization noise power / signal power} = 2 \cdot \left\{ \frac{K^2 \cdot (\tfrac{1}{2} - F(K))}{12 \cdot (2^{n-1} - 1)^2} \right\} \qquad (16)$$

and saturation noise (the clipping of overrange signals, dominant at high signal levels),

$$\text{saturation noise power / signal power} = 2 \cdot \left\{ (K^2 + 1) \cdot F(K) - \frac{K \cdot e^{-K^2/2}}{\sqrt{2\pi}} \right\}, \qquad (17)$$

where n is the number of bits and F(K) is the partial area under the normalized Gaussian curve (recall that the signal source is Gaussian),

$$F(K) = \frac{1}{\sqrt{2\pi}} \int_K^{\infty} e^{-x^2/2}\, dx. \qquad (18)$$

The NPR itself is the inverse of the sum of the power ratios in Eqs. (16) and (17), and is historically plotted versus the values of -20log(K). The ideal curves for 16-bit to 24-bit digitizers are shown in Figure 10.

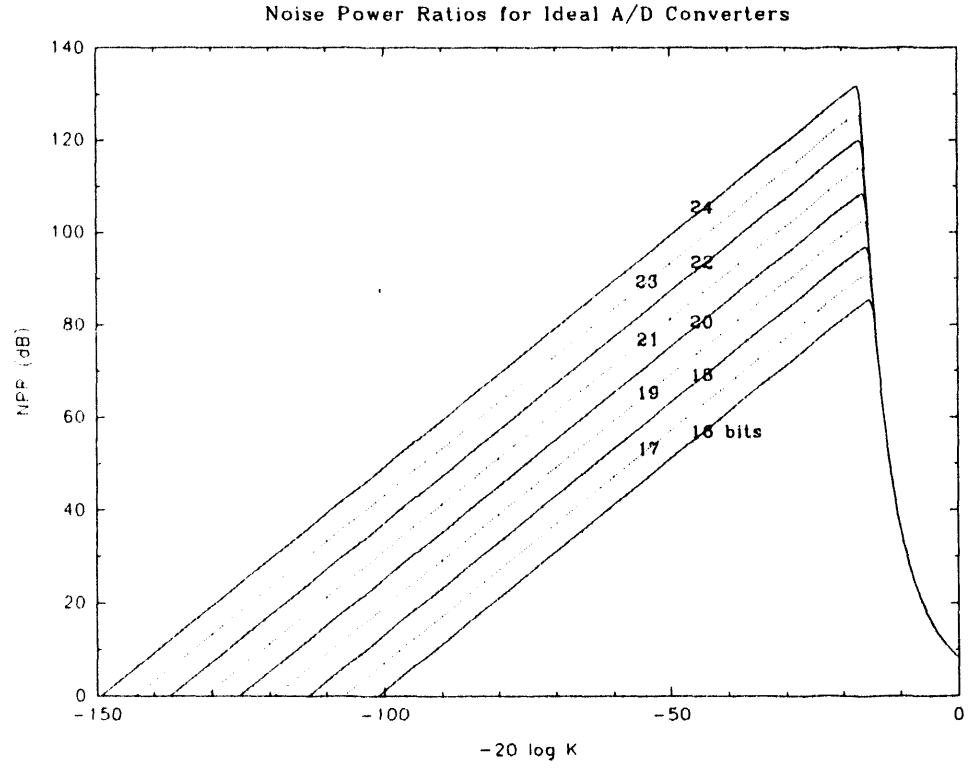

Figure 10 - NPR Curves for Ideal 16 to 24-Bit Digitizers

For the examples presented below the "digitizers" are simulated ideal n-bit systems (n=16, 20, and 24) with full-scale range of ±20 volts and 20 Hz sampling (T=0.05 second). Two data channels are produced; the second has a 0.1 volt DC offset, a 1 dB gain, and a

constant time shift, all relative to the first channel. The interpolation algorithm described in the previous section makes the procedure fairly insensitive to the magnitude of the time shift, but it should be noted that the values used ranged from 1% to 50% of the sampling time interval, T.

The simulated input signal was chosen to be Gaussian noise with approximately flat spectral content in the 0 to 5 Hz range, and sharply low-pass filtered with cutoff at 5 Hz. The power level in the passband was varied in 10 dB steps in order to get points approximating samples along the ideal NPR curves. Power values for the NPR were obtained by integrating the signal (either channel) and noise power spectral density estimates from 0 to 5 Hz.

In the first example, sample sets of simulated ideal digitizer data are compared to the non-digitized signal values. Since the signal is known, the appropriate noise model for this test configuration is the "lumped" noise model (Figure 2), and noise power estimates were obtained using Eq. (3). The results are shown in Figure 11 and illustrate the procedure for this special case.

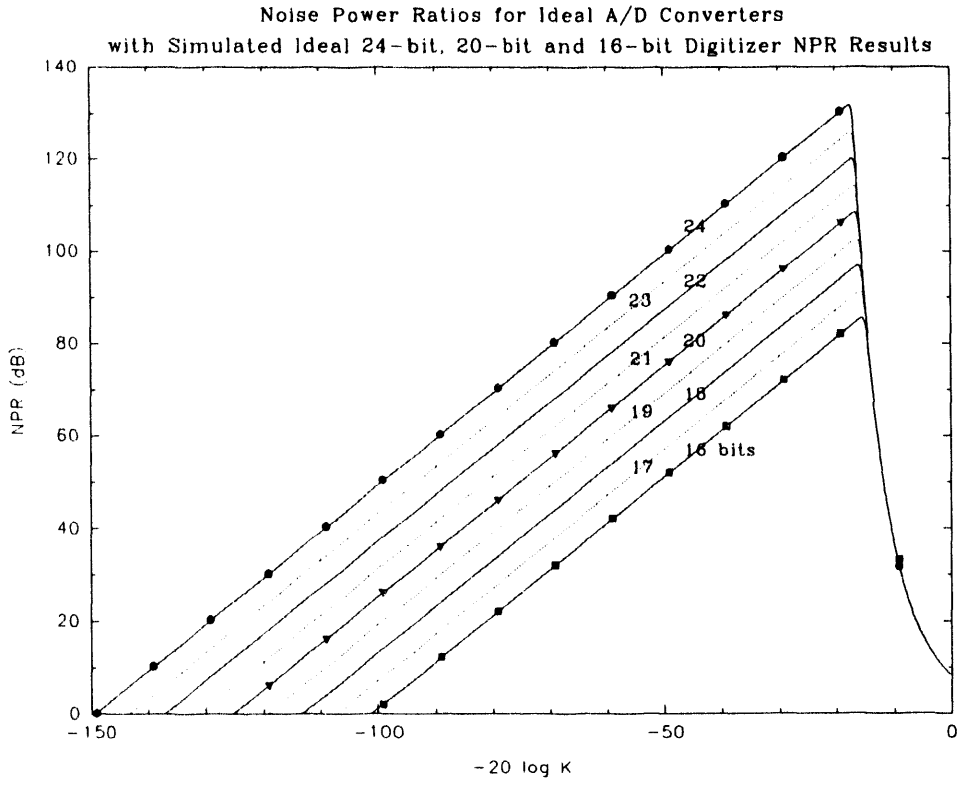

Figure 11 - NPR Estimation for Known Input (Lumped Noise Model)

The more useful application of NPR estimation would be to situations in which the input signal is known only generally, such as to frequency content and approximate amplitude range. The distributed noise model applies to this instance, and noise power estimation is via Eq. (12). Since signal power is also estimated from the digitized data, exact replication of ideal NPR's should not be expected, particularly in the region of clipped sampling (the "knee" in the ideal NPR curves around -20log(K) values of -15 to -20). This should not be much of a problem, since the points to the left of the knee and the location of the knee itself determine the broadband performance of the digitizer in terms of "NPR equivalent bits." In addition, clipped data is seldom considered to be of any value; a digitizer's performance to input beyond the full-scale values is generally unimportant so long as such overranges are identifiable.

The results of a simulation of the NPR procedure for ideal 16, 20, and 24-bit systems where the input signal power (as well as the noise power) is derived from the sampled data is presented in Figure 12. As expected, the results are not quite as good as in the first simulation; however, the errors in the unclipped data region (to the left of the knee) are always only a fraction of a bit. Repeated simulations of this test configuration utilizing different channel-to-channel gain and time shift values, as well as different DC offset values and number of digitized bits has shown that "NPR equivalent bits" can be consistently estimated to within ¼ bit, even when the input signal power must be inferred from the sampled data, and the error is always towards slightly underestimating the digitizer performance.

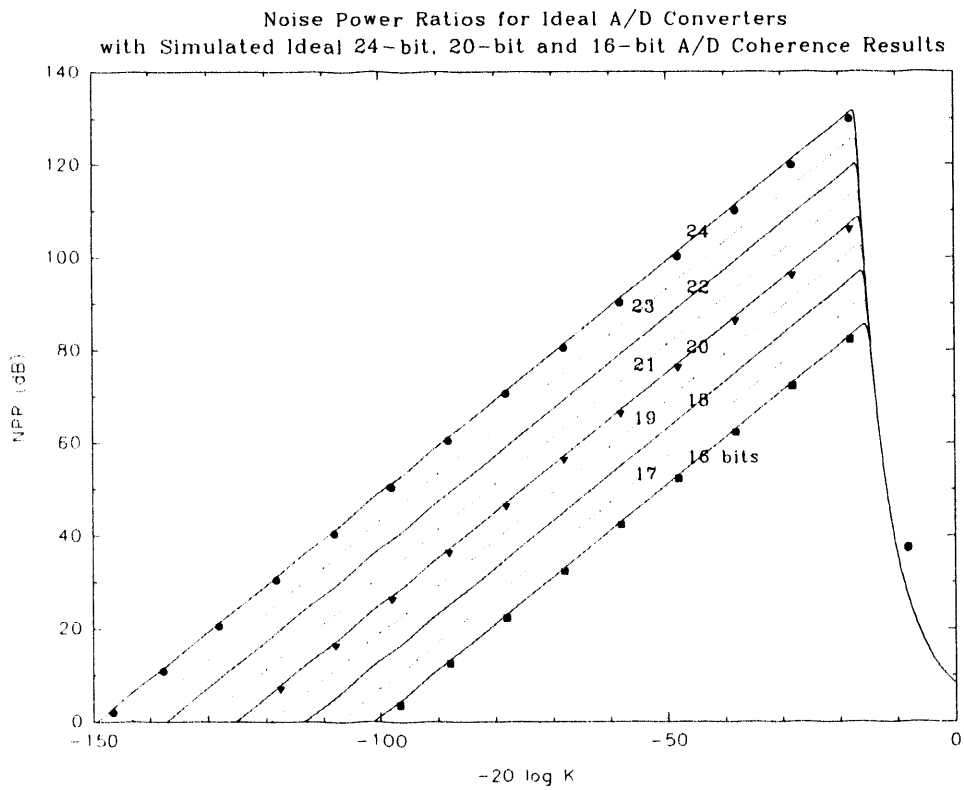

Figure 12 - NPR Estimation for Unknown Input (Distributed Noise Model)

Examples Using Actual High Resolution Digitizers

The coherence-based NPR measurement techniques have been applied to data acquired from three HRD system types, each with multi-channel, synchronous-sampling capability. The results are presented below and illustrate the usefulness of this method in evaluating broadband digitizer performance.

The first type, digitizer "A", has a full-scale voltage range of ± 20 volts and samples at a rate of 40 samples per second. Data samples are 24-bit integers (bit weight or scale factor is approximately 2.38 micro volts), and the manufacturer claims 22 bits of linearity, which, if correct, should match the NPR test results.

This system demonstrated a constant channel-to-channel sampling time offset of a few tens of microseconds (different for each pair). The interpolation scheme described earlier was used to align the data samples for the coherence analysis. In fact, the data sets used to illustrate the interpolation scheme were acquired for this test. Note from Figure 4 that the input signal was broadband and had flat power from 0 to about 16 Hz. Power values were obtained by integrating the signal and noise power spectral density estimates that result from the coherence analysis over the range of 0 to 18 Hz, the approximate range of high coherence values. The upper limit of integration of 18 Hz is not critical; however, the noise power near the Nyquist frequency of 20 Hz (see Figure 8) should not be included in the total noise power, since this power is largely computationally induced, due to the low input signal power in this range leading to low coherence estimates.

The NPR samples resulting from different input signal levels are plotted in Figure 13 along with the curves for ideal 16-bit to 24-bit systems for comparison. Digitizer "A" consistently demonstrates better than 22 bits of linearity. Since the NPR technique tends

to underestimate (slightly) the performance of digitizers, the manufacturer's claim of 22 bits of linearity is verified, and may be a "bit" conservative.

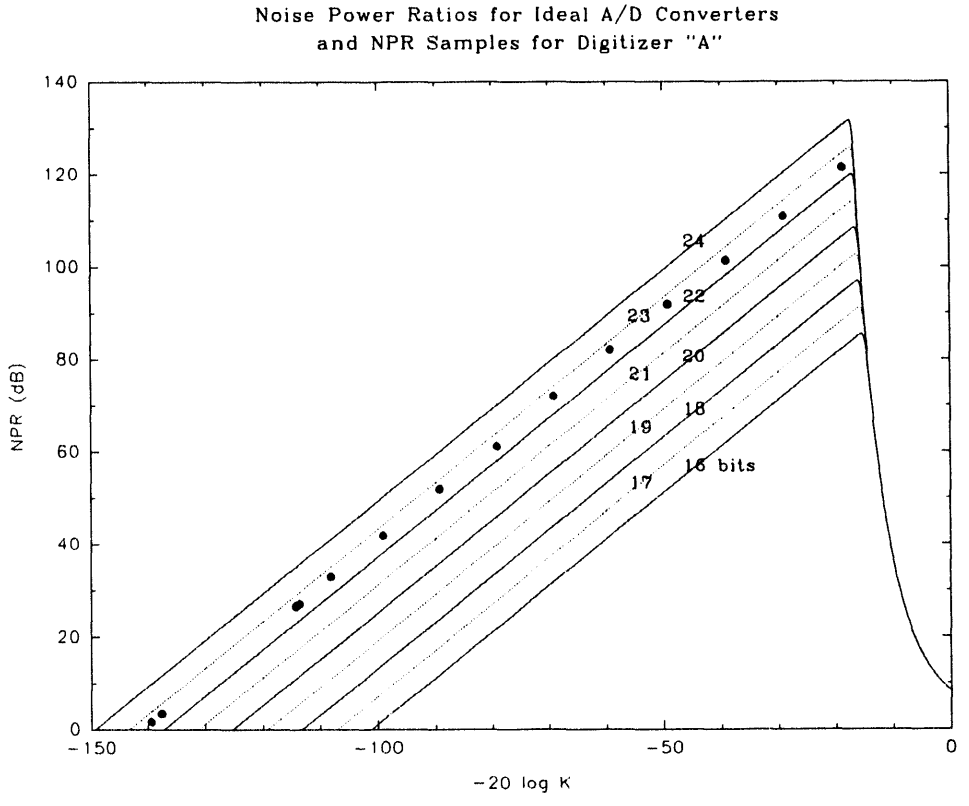

Figure 13 - Noise Power Ratio Samples for a 22-to-23-bit Digitizer

A second digitizer system "B" underwent a similar test and analysis, except that the interpolation scheme was not used, since channels appeared to be sampled virtually simultaneously. Again, a sample rate of 40 samples per second was used. Samples were 32 bit integers with a bit weight of approximately 1.90 micro volts, but the full-scale range of this system was ±10 volts, implying that only 23 bits were required.

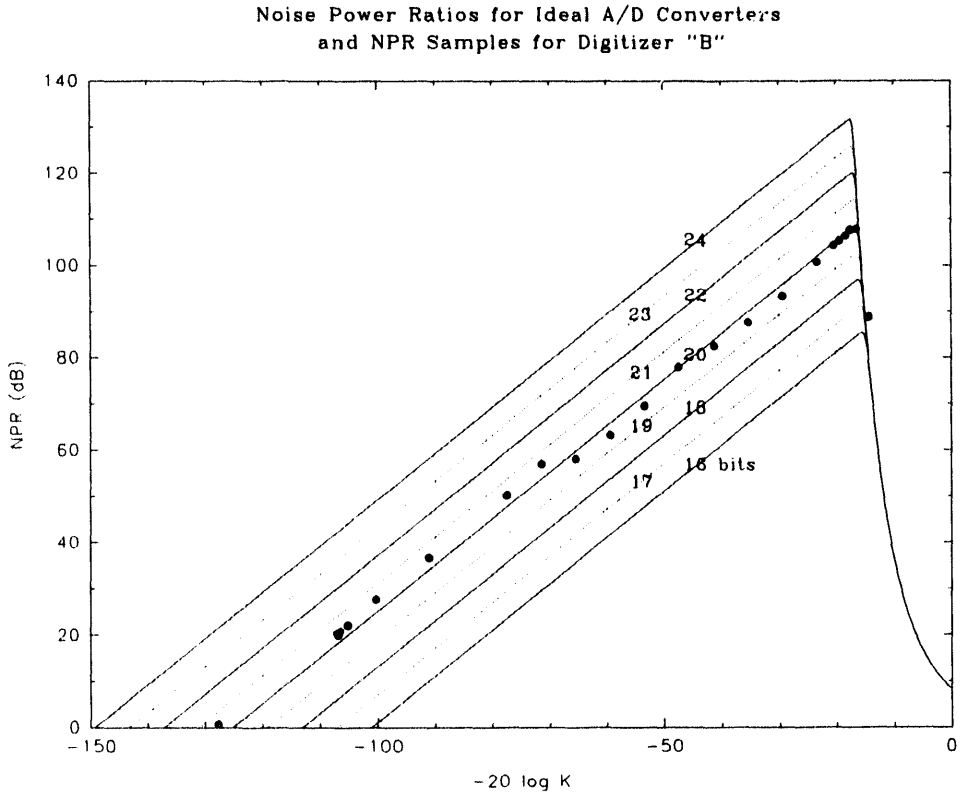

Figure 14 - Noise Power Ratio Samples for a 19-to-21-bit Digitizer

This manufacturer's claim of 20 bits of linearity is largely supported by the NPR samples shown in Figure 14. The degradation of the digitizer from 20-to-21-bit linearity for low-level signals (leftmost points) to a 19-to-20-bit system for higher input signals is fairly common for digitizers and often much worse than that demonstrated here. It is simply due to noise power rising with signal power. The cause can be very difficult to determine, but coherence-derived noise estimation is a tool which can make isolating a troublesome component possible, by substituting a questionable part and repeating the test at an input signal power level known to have previously produced unsatisfactory results.

An extreme case of degradation of performance with rising signal power involves a third digitizer, system "C", which has the same range, sample rate, and bit weight as digitizer "A". Figure 15 shows that this system has about 22 bits of linearity for low-level signals,

but suddenly degrades to an erratic 18-to-20-bit performance level for large signals. The break occurs when the RMS input signal value is approximately 2% of positive full scale. This severe characteristic is typical of gain-ranged systems, which achieve a large dynamic range with limited linearity.

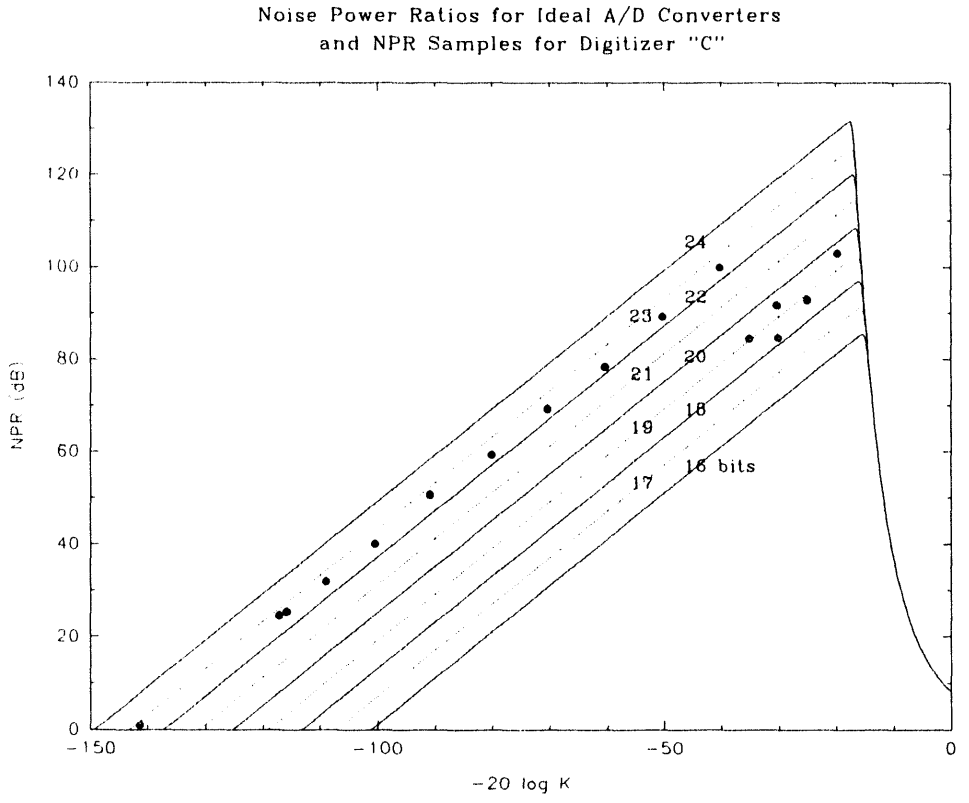

Figure 15 - Noise Power Ratio Samples for an Amplitude-Sensitive Digitizer

Conclusions

When the signal driving a given device is inadequately known in order for traditional system identification methods to be used, the determination of the self-noise spectrum of that device can be made possible through side-by-side testing and coherence analysis. This situation is often encountered with high resolution digitizers, since these instruments are more precise than the signal sources commonly available.

Some precautions are necessary when applying coherence analysis techniques to high resolution data. The first is to use a significantly precise computer floating point data type for the analyses; usually double precision is adequate. Another is less obvious: the cross-power spectral estimation involved in the coherence analysis is sensitive to misalignment of the data samples caused by different HRD data channels sampling at different times, even when this misalignment is only a few percent of the sampling interval. This problem can be overcome in one of several ways. In particular, an interpolation scheme that aligns the data samples while preserving frequency content was described and was shown to identify and compensate such misalignment.

The Noise Power Ratio is a useful technique for measuring system performance at a given frequency for low-resolution digitizers, but its application to the evaluation of high resolution systems is hampered by the lack of sufficiently quiet analog notch filters. However, a slight re-definition of the NPR using the signal and noise spectral estimates that result from coherence analysis eliminates the necessity of a high quality notch filter and has the added benefit of providing a broadband and possibly application-specific performance measurement. The equipment required for such analysis is commonly available, and the computational procedures are fairly straightforward.

References

Carter, G.C., Knapp, C.H., and Nuttall, A.H. (1973), "Estimation of the Magnitude-Squared Coherence Function Via Overlapped Fast Fourier Transform Processing", *IEEE Transactions on Audio and Electroacoustics*, Vol. AU-21, pp. 337-344.

Carter, G.C., and Nuttall, A.H. (1976), "Bias of the Estimate of Magnitude-Squared Coherence", *IEEE Transactions on Acoustics, Speech, and Signal Processing*, Vol. ASSP-24, pp. 582-583.

Carter, G.C. (1980), "Bias in Magnitude-Squared Coherence Estimation Due to Misalignment", *IEEE Transactions on Acoustics, Speech, and Signal Processing*, Vol. ASSP-28, pp. 97-99.

Durham, H.B. (1982), "Incoherence of Seismic Signals from Closely Spaced KS-36000 Seismometers", Sandia National Laboratories System Research Report.

Durham, H.B. (1987), "Initial Test and Evaluation of the S3 Seismometer", Sandia National Laboratories In-Country Seismic Verification Program Report.

Freeman, R.L. (1981), *Telecommunication Transmission Handbook* (Second Edition), John Wiley & Sons, pp. 215-221.

Goldsmith, S.Y. (1990), "Systematic Errors in Coherence Measurements on Parallel Sensors", Sandia National Laboratories In-Country Seismic Verification Program Report.

Gray, G.A., and Zeoli, G.W. (1971), "Quantization and Saturation Noise Due to Analog-to-Digital Conversion", *IEEE Transactions on Aerospace and Electronic Systems*, Vol. AES-7, pp. 222-223.

Holcomb, L.G. (1989), "A Direct Method for Calculating Instrument Noise Levels in Side-by-Side Seismometer Evaluations", United States Geological Survey Open-File Report 89-214.

Kester, W. (1989), "Noise Power Ratio Testing", Analog Devices, Inc., High Speed Data Seminar, pp. 1-76 to 1-79.

McDonald, T.S. (1977), *Frequency Domain Considerations of Numerical Integration Techniques*, Ph.D. Dissertation, The University of New Mexico, Department of Electrical Engineering and Computer Science.

Stearns, S.D. (1975), *Digital Signal Analysis*, Hayden.

Stearns, S.D. (1979), "Applications of the Coherence Function in Comparing Seismometers", Sandia National Laboratories Report 79-1633.

Stearns, S.D. (1981), "Tests of Coherence Unbiasing Methods", *IEEE Transactions on Acoustics, Speech, and Signal Processing*, Vol. ASSP-29, pp. 321-323.

Stearns, S.D., and David, R.A. (1993), *Signal Processing Algorithms Using Fortran and C*, Prentice Hall, pp. 67-74.

Stearns, S.D., and Hush, D.R. (1990), *Digital Signal Analysis* (Second Edition), Prentice Hall, pp. 80-85.

Welch, P.D. (1967), "The Use of Fast Fourier Transform for the Estimation of Power Spectra", *IEEE Transactions on Audio and Electroacoustics*, Vol. AU-15, pp. 70-73.

Distribution:

2 Dr. Jack Carrel and Paul Passmore
Refraction Technology, Inc.
2626 Lombardy Lane, Suite 105
Dallas, TX 75220

1 Dr. Theodore Cherry
Science Horizons, Inc.
710 Encinitas Boulevard, Suite 200
Encinitas, CA 92024

2 Gordon Cumming and R. Joseph Woodward
Chesapeake Sciences, Inc.
191 Main Street
Annapolis, MD 21401

1 Major Sean Doran
HQ AFTAC/TTS
Building 989
Patrick AFB, FL 32925

1 Fred E. Followill
Lawrence Livermore National Laboratories
Mail Stop 208
P.O. Box 808
Livermore, CA 94550

1 James C. Fowler
The IRIS Consortium
1616 North Fort Myer Drive
Arlington, VA 22209

1 Professor Eugene Herrin
Geophysics Department
Heroy Building
Southern Methodist University
Dallas, TX 75275

2 Dr. C. Robert Hutt and L. Gary Holcomb
USGS Seismic Laboratory
Building 10,002
Kirtland AFB East
Albuquerque, NM 87115

2 Theron Jensen and Dr. David Melgaard
J & M Systems, Ltd.
15100 Central SE
Albuquerque, NM 87123

1 Steven E. Pauley
Digital Technology Associates, Inc.
1330-A Galaxy Way
Concord, CA 94520

1 Robert Schendel
Texas Components Corporation
1716 West Sam Houston Parkway North
Houston, TX 77043

1 T. Michael Souders
National Institute of Standards and Technology
Building 220, Room B-162
Gaithersburg, MD 20899

1 O. D. Starkey
ODS Enterprises
1134 Easton Road
Dallas, TX 75218

1 Dr. Joseph M. Steim
Quanterra, Inc.
325 Ayer Road
Harvard, MA 01451-1132

1 Dr. Brian W. Stump
Los Alamos National Laboratory
P.O. Box 1663
MS C335
Los Alamos, NM 87545

1	MS 0365	1042	O. M. Solomon, Jr.
1	MS 0979	9204	L. S. Walker
20	MS 0655	9236	P. B. Herrington D. R. Breding E. P. Chael J. P. Claasen B. H. Corbell R. P. Fleming R. P. Kromer (3) T. S. McDonald (10) J. W. Walkup
1	MS 1159	9311	H. D. Garbin S. D. Stearns
1	MS 9018	8523-2	Central Technical Files
5	MS 0899	7141	Technical Library
1	MS 0619	7151	Technical Publications
10	MS 1119	7613-2	Document Processing For DOE/OSTI

DATE FILMED

7/6/94

END